

1 **Orbital, tectonic and oceanographic controls on Pliocene climate**
2 **and atmospheric circulation in Arctic Norway**

3 Sina Panitz¹, Ulrich Salzmann¹, Bjørg Risebrobakken², Stijn De Schepper², Matthew J.
4 Pound¹, Alan M. Haywood³, Aisling M. Dolan³, Daniel J. Lunt⁴

5 ¹Department of Geography and Environmental Sciences, Faculty of Engineering and
6 Environment, Northumbria University, Newcastle upon Tyne NE1 8ST, UK,
7 ulrich.salzmann@northumbria.ac.uk, matthew.pound@northumbria.ac.uk

8 ²Uni Research Climate, Bjerknes Centre for Climate Research, Jahnebakken 5, 5007 Bergen,
9 Norway, bjorg.risebrobakken@uni.no, stijn.deschepper@uni.no

10 ³School of Earth and Environment, University of Leeds, Woodhouse Lane, Leeds LS2 9JT,
11 UK, A.M.Haywood@leeds.ac.uk, A.M.Dolan@leeds.ac.uk

12 ⁴School of Geographical Sciences, University of Bristol, University Road, Bristol BS8 1SS,
13 UK, D.J.Lunt@bristol.ac.uk

14 **Corresponding author:** Sina Panitz (E-mail: sina.panitz@gmail.com)

15 **Abstract**

16 During the Pliocene Epoch, a stronger-than-present overturning circulation has been invoked
17 to explain the enhanced warming in the Nordic Seas region in comparison to low to mid-
18 latitude regions. While marine records are indicative of changes in the northward heat
19 transport via the North Atlantic Current (NAC) during the Pliocene, the long-term terrestrial
20 climate evolution and its driving mechanisms are poorly understood. We present the first
21 two-million-year-long Pliocene pollen record for the Nordic Seas region from Ocean Drilling
22 Program (ODP) Hole 642B, reflecting vegetation and climate in Arctic Norway, to assess the

23 influence of oceanographic and atmospheric controls on Pliocene climate evolution. The
24 vegetation record reveals a long-term cooling trend in northern Norway, which might be
25 linked to a general decline in atmospheric CO₂ concentrations over the studied interval, and
26 climate oscillations primarily controlled by precession (23 kyr), obliquity (54 kyr) and
27 eccentricity (100 kyr) forcing. In addition, the record identifies four major shifts in Pliocene
28 vegetation and climate mainly controlled by changes in northward heat transport via the
29 NAC. Cool temperate (warmer than present) conditions prevailed between 5.03–4.30 Ma,
30 3.90–3.47 Ma and 3.29–3.16 Ma and boreal (similar to present) conditions predominated
31 between 4.30–3.90 Ma, 3.47–3.29 and after 3.16 Ma. A distinct decline in sediment and
32 pollen accumulation rates at c. 4.65 Ma is probably linked to changes in ocean currents,
33 marine productivity and atmospheric circulation. Climate model simulations suggest that
34 changes in the strength of the Atlantic Meridional Overturning Circulation during the Early
35 Pliocene could have affected atmospheric circulation in the Nordic Seas region, which would
36 have affected the direction of pollen transport from Scandinavia to ODP Hole 642B.

37 *Keywords:* pollen, vegetation, Pliocene, North Atlantic Current, Central American Seaway

38 **1. Introduction**

39 During the Pliocene Epoch (5.33–2.59 Ma), global mean annual temperatures were 2–3°C
40 warmer than present (Haywood et al., 2013). Due to positive feedback mechanisms in the
41 Arctic, warming was particularly pronounced at high latitudes (Dowsett et al., 2013). On the
42 land masses surrounding the Nordic Seas, cool temperate and boreal forests reached further
43 north during the Pliocene into regions that are presently covered by subarctic boreal forests
44 and Arctic tundra (Bennike et al., 2002; Panitz et al., 2016; Verhoeven et al., 2013; Willard,
45 1994). The enhanced warming in the Nordic Seas region has been ascribed to a stronger than
46 present Atlantic Meridional Overturning Circulation (AMOC) and thus North Atlantic

47 Current (NAC) (Haug et al., 2001; Raymo et al., 1996, 1992). However, an increase in the
48 strength of the AMOC during the Pliocene is not simulated by all climate models (Zhang et
49 al., 2013). In both marine and terrestrial climate model simulations for the Pliocene,
50 temperatures are underestimated at high latitudes and remain below temperatures based on
51 data reconstructions (Dowsett et al., 2013; Salzmann et al., 2013). Palaeogeographic
52 differences have been suggested to account for the data-model mismatch. Simulations with an
53 altered palaeogeography (North Atlantic and Baltic river input, lowered Greenland-Scotland
54 Ridge and exposed Barents Sea) show a strong high latitude warming and weaker AMOC
55 (Hill, 2015). Closing the Bering Strait and the Canadian Arctic Archipelago has been shown
56 to increase warming at high latitudes and to strengthen the AMOC (Otto-Bliesner et al.,
57 2017). Model experiments to assess Pliocene terrestrial temperature change indicate that high
58 insolation, increased CO₂ concentrations and a closed Arctic gateway enhance high-latitude
59 warming (Feng et al., 2017). However, the low resolution and poor age control of most
60 terrestrial records limit the quantification of data-model mismatch at high latitudes (Feng et
61 al., 2017).

62 Heat is transported to the Arctic Ocean via the Norwegian Atlantic Current (NwAC), the
63 continuation of the NAC in the eastern Nordic Seas. Pliocene marine records of sea surface
64 temperature (SST) and palaeoceanographic changes in the North Atlantic and Nordic Seas
65 indicate repeated variations in the northward heat transport via the NAC (Bachem et al.,
66 2017; De Schepper et al., 2013; Lawrence et al., 2009; Naafs et al., 2010; Risebrobakken et
67 al., 2016). The development of a modern-like surface ocean circulation in the Nordic Seas
68 around 4.5 Ma has been linked to the establishment of a northward flow through the Bering
69 Strait and a shoaling of the Central American Seaway (CAS) (De Schepper et al., 2015). In
70 Ocean Drilling Program (ODP) Hole 642B increased abundances of the dinoflagellate species
71 *Protoceratium reticulatum* after 4.2 Ma suggest increased Atlantic water influence at the site

72 and the establishment of a modern-like NwAC (De Schepper et al., 2015). Alkenone-derived
73 SSTs in Hole 642B show a pronounced cooling at 4.3 Ma, with temperature decreasing by
74 $\sim 5^{\circ}\text{C}$ to values fluctuating around the Holocene average, which might be linked to a
75 strengthening of the East Greenland Current (EGC) and reduced amplitude of obliquity
76 forcing (Bachem et al., 2017). Carbon isotope changes in Hole 642B are indicative of a well-
77 ventilated Norwegian Sea comparable to the present situation (Risebrobakken et al., 2016).
78 Increasing surface water densities have been inferred at the same site which may be the result
79 of increased Atlantic water influence already from 4.6 Ma (Risebrobakken et al., 2016). Early
80 Pliocene oceanographic changes in the Caribbean indicate that the shoaling of the CAS
81 between 4.8 and 4.0 Ma is associated with a strengthening of the AMOC (Groeneveld et al.,
82 2008; Haug et al., 2001; Osborne et al., 2014; Steph et al., 2010). However, benthic carbon
83 and oxygen isotope records from the Atlantic suggest that deep water circulation remained
84 unaffected by the shoaling of the CAS (Bell et al., 2015). Neogene palaeofloras from North
85 America and Western Eurasia indicate that the difference in the thermal gradients between
86 these two continents developed between the late Miocene and late Pliocene, possibly in
87 response to the intensification of the AMOC after the shoaling of the CAS during the early
88 Pliocene (Utescher et al., 2017). A pronounced warming in the Norwegian Sea took place
89 around 4.0 Ma in response to a strengthened northward heat transport potentially due to the
90 CAS shoaling or a deepening of the Greenland-Scotland Ridge (Bachem et al., 2017). The
91 presence of a warmer NwAC is supported by a corresponding depletion of planktic $\delta^{18}\text{O}$ in
92 Hole 642B (Risebrobakken et al., 2016). Contemporaneous cooling in the Iceland Sea
93 resulted in the establishment of a strong zonal gradient and strengthened surface circulation
94 in the Nordic Seas (Bachem et al., 2017; Herbert et al., 2016). The presence of warm surface
95 waters in the Norwegian Sea might have contributed, in addition to regional tectonic uplift, to
96 the development of seasonal sea ice in the Eurasian sector of the Arctic Ocean around 4 Ma

97 (Knies et al., 2014) by enhancing evaporation and precipitation, and thus Arctic freshwater
98 supply (Bachem et al., 2017). The impact of these palaeoceanographic changes on the
99 terrestrial climate evolution in northern Norway and potential links to the shoaling of the
100 CAS are unknown.

101 For the Late Pliocene (Piacenzian, 3.60–2.58 Ma), SST reconstructions show a variable
102 pattern in the magnitude of warming, with the largest anomalies being recorded in the Iceland
103 and Greenland Seas (Dowsett et al., 2013; Knies et al., 2014; Schreck et al., 2013) and the
104 lowest in the Norwegian Sea (Bachem et al., 2017, 2016). Decreasing SSTs in the Norwegian
105 Sea between 3.65 and 3.30 Ma are suggested to be the result of a reduced influence of the
106 NAC on the NwAC (Bachem et al., 2017). A new multi-proxy study shows that during the
107 Piacenzian vegetation and climate changes in northern Norway coincide with variations in
108 Atlantic water influence and SST changes in the Norwegian Sea (Panitz et al., 2017).

109 Whereas most Pliocene terrestrial records show warmer-than-present climatic conditions, the
110 reconstruction of terrestrial climate evolution and variability before the onset of extensive
111 Pleistocene Northern Hemisphere Glaciation (NHG) has, however, been hampered by the
112 short temporal coverage of existing records in the Nordic Seas region (Bennike et al., 2002;
113 Verhoeven et al., 2013; Willard, 1994). Here, we investigate the relation between Pliocene
114 oceanographic changes in the North Atlantic and Nordic Seas and terrestrial climate changes
115 in northern Norway over a two-million-year long time period.

116 This study presents a Pliocene (5.03–3.14 Ma) high-resolution pollen record for the Nordic
117 Seas region, reflecting vegetation changes in northern Norway. The new Early Pliocene
118 pollen record from ODP Hole 642B is combined with the previously published Late Pliocene
119 pollen record from the same site (Panitz et al., 2016) and compared to SST and water mass
120 changes in the Norwegian Sea (Bachem et al., 2017; De Schepper et al., 2015; Risebrobakken
121 et al., 2016). Climate model output is presented to assess potential changes in pollen transport

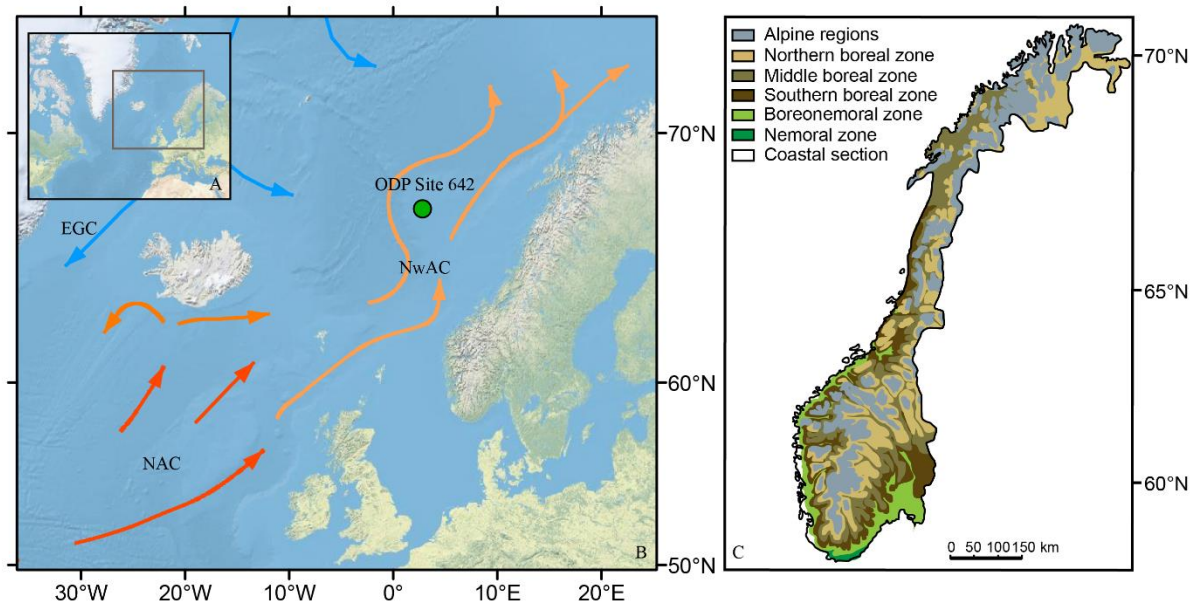


Figure 1: Location of (A) the study area in the North Atlantic and (B) ODP Hole 642B in the Norwegian Sea. (C) Modern vegetation of Norway modified after Moen (1987). In (B), colour coding of currents indicates the relative temperature: dark orange = warm; light orange = moderately warm; blue = cold. EGC = East Greenland Current, NAC = North Atlantic Current and NwAC = Norwegian Atlantic Current.

122 to the site by wind in response to changes in AMOC strength due to the shoaling of the CAS.
 123 The aim of this study is to assess (1) the long-term controls on vegetation and climate
 124 changes in northern Norway, (2) the response of vegetation changes to the variability of the
 125 NAC, and (3) the potential effects of early Pliocene oceanographic changes on pollen
 126 transport to the site.

127 **2. Oceanographic setting and modern vegetation of Norway**

128 ODP Hole 642B was recovered during Leg 104 and is situated about 400–450 km off the
 129 coast of Norway on the outer Vøring Plateau in the Norwegian Sea (67°13.2'N, 2°55.8'E,
 130 1286 m water depth, Shipboard Scientific Party (1987); Figure 1). A branch of the NwAC,
 131 which is an extension of the warm NAC, flows northward on either side of the plateau (Orvik
 132 and Niiler, 2002). At present, the influence of these warm waters results in relatively mild
 133 climatic conditions in Scandinavia (Furevik, 2000). Boreal forest extends over most of

134 Norway with pure deciduous forests only found along the south coast. The proportion of
135 deciduous and thermophilic elements decreases with increasing latitude, and altitude of the
136 Scandinavian mountains (Moen, 1987). In southern Scandinavia, the altitudinal limit of the
137 tree line is reached at ~1200 m above sea level, with alpine tundra predominating beyond the
138 tree limit (Moen, 1999). The tree line steadily declines with increasing latitude until tundra
139 prevails at sea level in northernmost Norway (Moen, 1999, 1987). Based on the analysis of
140 two (sub)surface samples from Hole 642B, the pollen signal has been shown to be
141 representative of the prevailing vegetation in northern Norway (Panitz et al., 2016). The
142 predominance of wind-pollinated taxa in the (sub)surface and Pliocene samples suggests that
143 pollen is mainly transported to the site by wind. While plumes of cold fjord water enter the
144 Norwegian Sea during spring at present and extend up to 100 km offshore (Mork, 1981), such
145 plumes most likely did not develop during the Pliocene due to the absence of fjords and a
146 reduced ice cover. There is no evidence of the existence of large rivers during the Pliocene,
147 with modest sedimentation along the Norwegian continental margin during the Middle
148 Eocene to Pliocene. Sedimentation rates increased greatly with the onset of NHG around
149 2.6 Ma (Eidvin et al., 2000; Faleide et al., 2008).

150 **3. Materials and Methods**

151 **3.1. Age model**

152 The age model for the Pliocene section of ODP Hole 642B is based on the updated magnetic
153 stratigraphy of Bleil (1989) to the ATNTS2012 time scale (Hilgen et al., 2012) and
154 correlation of the benthic $\delta^{18}\text{O}$ curve from Hole 642B to the global LR04 benthic $\delta^{18}\text{O}$ stack
155 between 4.147 and 3.14 Ma (Lisiecki and Raymo, 2005; Risebrobakken et al., 2016). A major
156 hiatus exists in the Late Pliocene section of the record after 3.14 Ma (Bleil, 1989;
157 Risebrobakken et al., 2016). The tie points for the age model (Supplementary Table 1) are

158 shown alongside the sedimentation rate in Figure 3 (Risebrobakken et al., 2016), with
159 changes in sedimentation rate reflecting the position of the tie points.

160 **3.2. Sample preparation and pollen analysis**

161 A total of 128 samples were selected for pollen analysis between 83.55 and 66.95 metres
162 below sea floor (mbsf) from ODP Hole 642B, ranging in age from 5.03 to 3.14 Ma
163 (Risebrobakken et al., 2016). The samples were pre-sieved in Bergen, Norway through a
164 63 µm mesh to retain foraminifera for oxygen isotope analysis (Risebrobakken et al., 2016).
165 A potential bias in the pollen data due to the loss of larger Pinaceae grains has been excluded
166 by comparison of sieved and unsieved samples (Panitz et al., 2016). Sample preparation was
167 carried out at the Palynological Laboratory Services Ltd, North Wales and Northumbria
168 University, Newcastle, using standard palynological techniques (Faegri and Iversen, 1989). In
169 order to calculate pollen concentrations, one *Lycopodium clavatum* spore tablet was added to
170 each sample (Stockmarr, 1971). The treatment with cold HCl (20%) was followed by the use
171 of cold, concentrated HF (48%) to remove carbonates and silicates, respectively. An
172 additional wash with hot (c. 80°C) HCl (20%) was conducted to remove fluorosilicates. After
173 back-sieving the sediment through a 10 µm screen, the residue was mounted on glass slides
174 using glycerol-gelatine jelly. Pollen analysis was carried out using a Leica Microscope (DM
175 2000 LED) at magnifications of 400x and 1000x. The identification of pollen and spores was
176 aided by the pollen reference collection at Northumbria University and the use of literature
177 (e.g. Beug, 2004). Reworked pollen and spores were differentiated from in situ grains based
178 on the thermal maturity of the exine, with reworked grains having orange to brown colours,
179 and/or their presence outside their stratigraphic range. Particularly reworked gymnosperm
180 pollen showed a high degree of compression, a faint alveolar structure of the saccae and
181 mineral imprints (de Vernal and Mudie, 1989a, 1989b; Willard, 1996). In situ *Lycopodium*
182 *clavatum* spores differed in colour from the marker spores.

183 For the majority of samples more than 300 pollen and spore grains were counted. Only 20
 184 samples yielded a total count of less than 300 grains. Percentages of pollen and spores were
 185 calculated based on the pollen sum, excluding *Pinus* pollen as well as unidentified and
 186 reworked pollen and spores. The pollen sum excluding *Pinus* pollen regularly exceeds 170
 187 pollen and spores (for further detail see Supplementary Material). The software Tilia was
 188 used to generate pollen diagrams and perform stratigraphically constrained cluster analysis
 189 for the delimitation of pollen zones (Grimm, 1990, 1987). Pollen accumulation rates (PARs)
 190 were calculated based on the following formula:

191 (1)
$$PAR = C \times \rho \times S$$

192 with PAR in grains/(cm² kyr), *C* being the pollen concentration (grains/g dry weight), ρ the
 193 dry bulk density (g/cm³) and *S* the sedimentation rate (cm/kyr). PARs have been calculated to
 194 compensate for fluctuations in the sedimentation rate that can affect pollen concentrations
 195 (Traverse, 1988). Pollen and spore taxa have been bioclimatically grouped following the
 196 modern distribution of their nearest living relatives (Table 1).

197 Table 1: Pollen and spore taxa from ODP *Hole* 642B attributed to the bioclimatic zones
 198 plotted in Figure 6.

Bioclimate groups	Attributed pollen and spore taxa
Cool temperate forests	<i>Carpinus, Carya, Corylus, Ilex, Ostrya, Pterocarya,</i> <i>Quercus, Sciadopitys, Taxus, Tsuga, Ulmus</i>
Boreal forests	<i>Abies, Alnus, Betula, Cupressaceae, Juniperus, Picea</i>
Boreal and alpine peatlands and heathlands	<i>Asteraceae, Ericaceae, Lycopodium</i> spp., <i>Sphagnum</i>

199 **3.3. Time series analysis**

200 In order to detect cyclicity within the vegetation changes, a continuous wavelet transform was
201 carried out using a Morlet wavelet (Torrence and Compo, 1998). Due to the low pollen
202 counts between 4.56 and 4.37 Ma, we only analysed the time interval from 4.37 to 3.14 Ma.
203 For wavelet analysis, the unevenly spaced data was interpolated on 1000-year time steps prior
204 to analysis in PAST3. In order to test whether peaks in the spectrum are significant against
205 the red-noise background, we applied REDFIT (Schulz and Mudelsee, 2002). The analyses
206 were performed on the relative abundance of *Pinus* pollen which dominates throughout the
207 record.

208 **3.4. Climate model description**

209 Climate model output from the Hadley Centre coupled atmosphere-ocean climate model
210 (HadCM3, Gordon et al., 2000) has been used to assess potential changes in pollen transport
211 by wind to ODP Hole 642B in response to changes in AMOC strength, following the
212 shoaling of the CAS. Previous studies have shown that closing the CAS is an effective means
213 of increasing AMOC strength in a coupled atmosphere-ocean climate model (Lunt et al.,
214 2008a, 2008b). HadCM3 has been shown to reproduce the large scale features of Pliocene
215 climate (Haywood et al., 2013). It has been used for a number of Pliocene climate modelling
216 studies and was the first coupled atmosphere-ocean climate model (Haywood and Valdes,
217 2004) to run using boundary conditions defined by the PRISM project based at the US
218 Geological Survey.

219 The simulations shown here have used PRISM2 boundary conditions (following Dowsett et
220 al., 1999). In one experiment the CAS is specified as open (hereafter referred to as OCAS)
221 and the other the CAS is closed (hereafter referred to as CCAS; simulations are comparable
222 to those presented in (Lunt et al., 2008b). These changes were made to assess the potential
223 variability in AMOC strength on regional atmospheric circulation and pollen transport from

224 Scandinavia to ODP Hole 642B. We focus on the model output surface wind speeds and
225 atmospheric pressure during spring (March, April, May) as most plants disperse pollen during
226 that season.

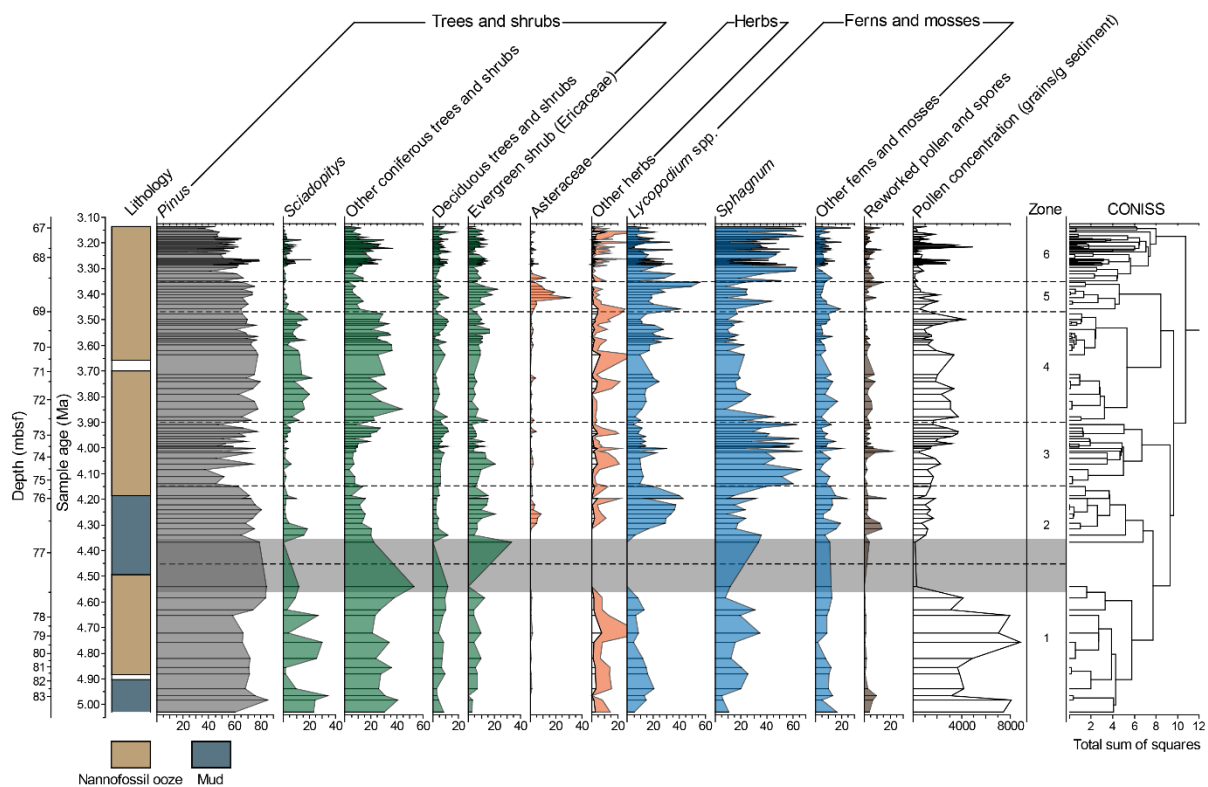
227 **4. Results**

228 **4.1. Pliocene pollen assemblages and vegetation reconstruction**

229 The Pliocene pollen record of ODP Hole 642B is divided into six pollen zones (Figure 2).
230 The complete pollen record is provided in Supplementary Material Figure 1.

231 **Pollen Zone 1**

232 The lowermost pollen zone (PZ 1, 83.55–77.38 mbsf, 5.03–4.51 Ma, 15 samples, two
233 samples at the top of the zone were excluded from relative abundance calculations shown in
234 Figure 2 due to low counts) is characterised by high abundances of *Pinus* pollen and other
235 boreal to temperate coniferous tree and shrub taxa (*Abies*, Cupressaceae, *Juniperus* type,
236 *Picea*, *Sciadopitys*, *Taxus* and *Tsuga*). Together with the occurrence of temperate deciduous
237 taxa (*Carpinus*, *Carya*, *Pterocarya* and *Quercus*), PZ 1 is indicative of the presence of
238 diverse cool temperate mixed forests in northern Norway (Figure 2). Fluctuations in the
239 proportions of the temperate taxon *Sciadopitys* suggest that the interval was interrupted by
240 cooler intervals that were more boreal in character. Notable are the very high pollen
241 concentrations throughout PZ1 that decrease markedly at the top of the zone (Figure 2). The
242 environmental interpretation of the pollen assemblages at the transition from PZ 1 to PZ 2 is
243 hampered due to low pollen counts. The presence of mainly boreal tree and shrub taxa
244 (*Alnus*, *Betula*, Ericaceae, *Fraxinus*, *Juniperus* type and *Pinus*) and mosses (*Huperzia* and
245 *Sphagnum*) may be an indication of the prevalence of boreal forests and tundra environments.



246

Figure 2: Abundances of pollen and spores and taxa groups in the Pliocene sediments of ODP Hole 642B. Coloured area for abundances of “other herbs” represents a 5-fold exaggeration of percentages (white area). Percentages of pollen and spores were calculated based on the pollen sum, excluding *Pinus*, unidentified and reworked pollen and spores. Only for the calculation of *Pinus* percentages were the counts of *Pinus* pollen included in the pollen sum. Depth is indicated in metres below sea floor (mbsf). Grey horizontal bar delimits samples with low pollen counts (<100). Samples with a total count of less than 40 grains are not shown. The lithology of the Pliocene section of Hole 642B was obtained from the original report (Shipboard Scientific Party, 1987).

247 The thermophilic but cold-tolerant taxon *Tsuga* is also present, presumably growing at
 248 favourable sites (see Supplementary Material).

249 **Pollen Zone 2**

250 In the middle part of pollen zone 2 (PZ 2, 76.60–75.29 mbsf, 4.30–4.15 Ma, 14 samples, two
 251 samples at the base of the zone were excluded from relative abundance calculations shown in
 252 Figure 2 due to low counts) the predominance of cool temperate forests is inferred from the
 253 relative high abundance of *Sciadopitys* pollen. The subsequent decrease in the percentages of

254 *Sciadopitys* pollen and increase in the relative proportion of Asteraceae and Ericaceae pollen
255 as well as *Lycopodium* spores (incl. *Lycopodium annotinum*, *Lycopodium clavatum*,
256 *Lycopodium inundatum* and *Lycopodium* spp.; Figure 2) is interpreted to reflect a southward
257 shift of cool temperate mixed forests and an opening of the vegetation at higher altitudes due
258 to a lowering of the treeline, leading to the development of alpine herb fields/heathlands
259 under a boreal climate.

260 **Pollen Zone 3**

261 At the beginning of pollen zone 3 (PZ 3, 75.29–72.60 mbsf, 4.15–3.90 Ma, 19 samples), the
262 relative abundance of *Pinus* pollen declines slightly whereas that of *Sphagnum* spores
263 markedly increases. In conjunction with low proportions of other coniferous trees and shrubs
264 taxa, these pollen assemblage changes suggest that boreal forest prevailed and peatlands
265 expanded due to further cooling and/or wetter conditions (Figure 2).

266 **Pollen Zone 4**

267 In pollen zone 4 (PZ 4, 72.60–69.02 mbsf, 3.90–3.47 Ma, 25 samples), pollen of *Pinus* and
268 other coniferous trees and shrubs predominate the assemblages, suggesting a re-establishment
269 of cool temperate climatic conditions in northern Norway (Figure 2).

270 **Pollen Zone 5**

271 After this prolonged warm interval, the proportions of Asteraceae and Ericaceae pollen and
272 *Lycopodium* spores increase in pollen zone 5 (PZ 5, 69.02–68.54 mbsf, 3.47–3.35 Ma, 9
273 samples, Figure 2), indicating an expansion of herb fields/heathlands at higher altitudes in
274 response to the establishment of cooler climatic conditions and an associated lowering of the
275 tree line. Together with the predominance of *Pinus* pollen and low abundances of other

276 coniferous trees and shrubs, this suggests that boreal forests and alpine herb fields/heathlands
277 prevailed in northern Norway under subarctic climatic conditions.

278 **Pollen Zone 6**

279 In the uppermost pollen zone (PZ 6, 68.54–66.95 mbsf, 3.35–3.14 Ma, 46 samples) the
280 overall decline in the relative abundance of *Pinus* pollen and increasing proportion of
281 *Sphagnum* spores is interpreted to represent the expansion of peatlands at the expense of
282 forests (Figure 2). Abundance peaks in the temperate taxon *Sciadopitys* point to reoccurring
283 warmer, and thus highly variable, climatic conditions (Panitz et al., 2016). Throughout PZ 2
284 to 6, pollen concentrations are relatively low in comparison to those within PZ 1 (Figure 2).

285 **4.2. Climate model results**

286 During Northern Hemisphere (NH) spring (March, April, May), model results for both
287 experiments indicate a predominantly westerly to southwesterly wind between 45°N and
288 ~65–70°N (Figure 4). Between ~65–70°N and 75°N the airflow is predominantly easterly in
289 the Nordic Seas. Whilst the dominant direction of flow south of ~65–70°N is predominantly
290 westerly to southwesterly, over the Scandinavian land mass the details of circulation are more
291 complex. In particular, we highlight in Figure 4 the region in central and northern
292 Scandinavia where there is a tendency for easterly flow. The tendency for easterly flow over
293 central and northern Scandinavia is enhanced in the OCAS scenario (Figure 4).

294 In the CCAS scenario, AMOC is increased relative to the OCAS scenario, with a
295 corresponding enhancement in ocean heat transport in the NH (see Lunt et al., 2008b). This in
296 turn alters the regional temperature and atmospheric pressure gradients over Northern Europe
297 and the Nordic Seas (Figure 4; Lunt et al., 2008b). The result of which is to encourage
298 stronger westerly and southwesterly flow (Figure 4), creating a corresponding suppression of
299 easterly flow from central and northern Scandinavia into the Nordic Seas in the CCAS

300 scenario (Figure 4). These results are most clearly expressed by surface wind and pressure
301 patterns (Figure 4), however we have examined the nature of circulation and pressure at
302 higher altitudes (not shown) in the atmosphere and in each case find the potential for easterly
303 flow from Scandinavia is enhanced in the weaker AMOC scenario (OCAS).

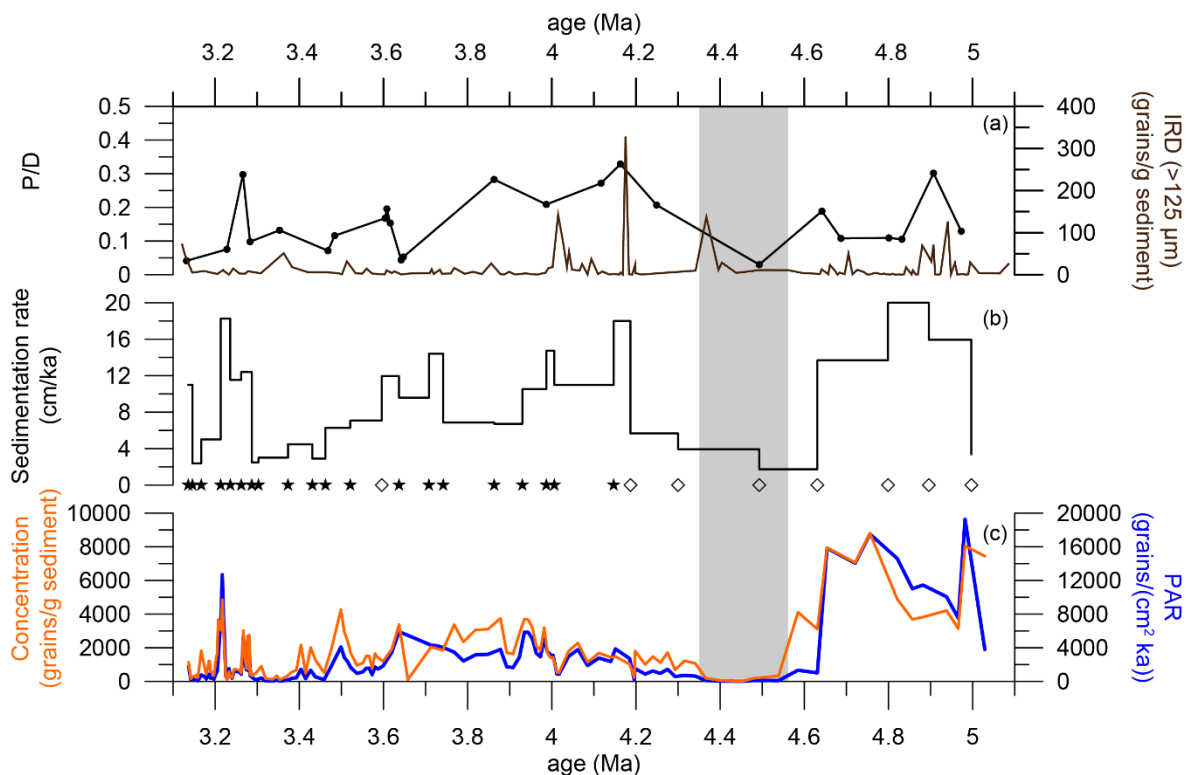
304 **5. Discussion**

305 **5.1. Pollen Accumulation Rates indicate changes in ocean and atmospheric** 306 **circulation at c. 4.6 Ma**

307 A distinct decline in sedimentation rate, pollen concentration and PAR at c. 4.65 Ma (Figure
308 2 and 3) suggests that changes in atmospheric circulation, ocean currents and/or taphonomic
309 processes may have affected the transport, deposition and/or preservation of pollen (e.g.
310 Dupont, 2011). The strong correlation between PARs, which takes fluctuations in
311 sedimentation rates into account, and sedimentation rates in our record suggests potential
312 changes in the sedimentary regime or source area. We can confidently discard any major
313 influence of fluvial sediment transport from the Scandinavian mainland during the Pliocene.
314 During the Oligocene to Pliocene, the inner Norwegian Sea continental shelf was the main
315 depocentre for sediments from western Scandinavia. Hemipelagic sediments were deposited
316 on the shelf and pelagic ooze on the slope and rise (Eidvin et al., 2014). West of the
317 continental shelf, pelagic sedimentation (biogenic ooze) accumulated during the Oligocene to
318 Pliocene (Eidvin et al., 2014). ODP Hole 642B is located ~450 km off the Norwegian coast at
319 a water depth of ~1300 meter below sea level on the Vøring plateau, which was unaffected
320 by sediment supply from Scandinavia. The Hole 642B pollen record also shows a low
321 pollen/dinocyst (P/D) ratio (Figure 3) and a dominance of long-distance, wind-pollinated taxa
322 (such as *Pinus*, Figure 2), both indicating a very low influence of sea level and sediment
323 accumulation changes, if compared to Quaternary glacials and interglacials (McCarthy et al.,

324 2003; McCarthy and Mudie, 1998). The pollen record does not show any change in the
325 proportions of reworked pollen grains or a shift in vegetation composition at 4.65 Ma (Figure
326 2), indicating that preservation issues or changes in pollen production on the mainland are an
327 unlikely cause for the decline in PAR.

328 At Hole 642B, stable carbon isotope values indicate an increase in bottom water ventilation
329 between 4.65 and 4.40 Ma, reaching values closer to the Holocene mean (Risebrobakken et
330 al., 2016). A decline in dinocyst and acritarch accumulation rates suggests a
331 contemporaneous reduction in primary productivity (De Schepper et al., 2015), which might
332 have affected the sinking of pollen grains to the sea floor (Dupont, 2011). These
333 oceanographic changes broadly coincide with the deep subsidence of the Hovgård Ridge in
334 the Fram Strait and the shoaling of CAS, with the latter resulting in an increased AMOC
335 (Haug et al., 2001; Risebrobakken et al., 2016; Steph et al., 2010). The Neogene AMOC and
336 its varying intensity prior to the closure of CAS during the Early Pliocene is a matter of
337 debate. Modelling results indicate that both oceanographic circulation and associated heat
338 transport were considerably reduced with an open CAS when compared to present-day
339 conditions (e.g. Lunt et al., 2008b), whereas palaeobotanical evidence suggests a Pliocene
340 steepening of the shallow thermal latitudinal gradients that existed in North America and
341 Western Eurasia throughout the Miocene (Utescher et al., 2017). These changes might have
342 also influenced the predominant mode of pollen transport which largely depends on the
343 regional climate and the distance of the site from the source area (Mudie and McCarthy,
344 2006). Today, the main atmospheric circulation pattern in the North Atlantic region is
345 determined by the difference in pressure between the subtropical Azores high and the
346 subpolar Icelandic low (Furevik, 2000). During the early Zanclean, atmospheric circulation
347 changes in the Nordic Seas region might have occurred in response to the shoaling of the
348 CAS and its effect on the AMOC (Haug et al., 2001; Steph et al., 2010).



350

351 **Figure 3:** Sedimentological data from ODP Hole 642B. (a) pollen (P) and dinoflagellate cyst
 352 (D) ratio (De Schepper et al., 2015) and ice rafted debris (IRD) (Jansen et al., 1990); (b)
 353 sedimentation rate and age control points based on magnetic reversals (diamonds) and
 354 correlation of the benthic $\delta^{18}\text{O}$ values to the LR04 global benthic $\delta^{18}\text{O}$ stack (stars)
 355 (Risebrobakken et al., 2016); (c) pollen concentrations and pollen accumulation rates (PARs)
 356 (this study). Grey horizontal bar delimits samples with low pollen counts (<100).

357

358

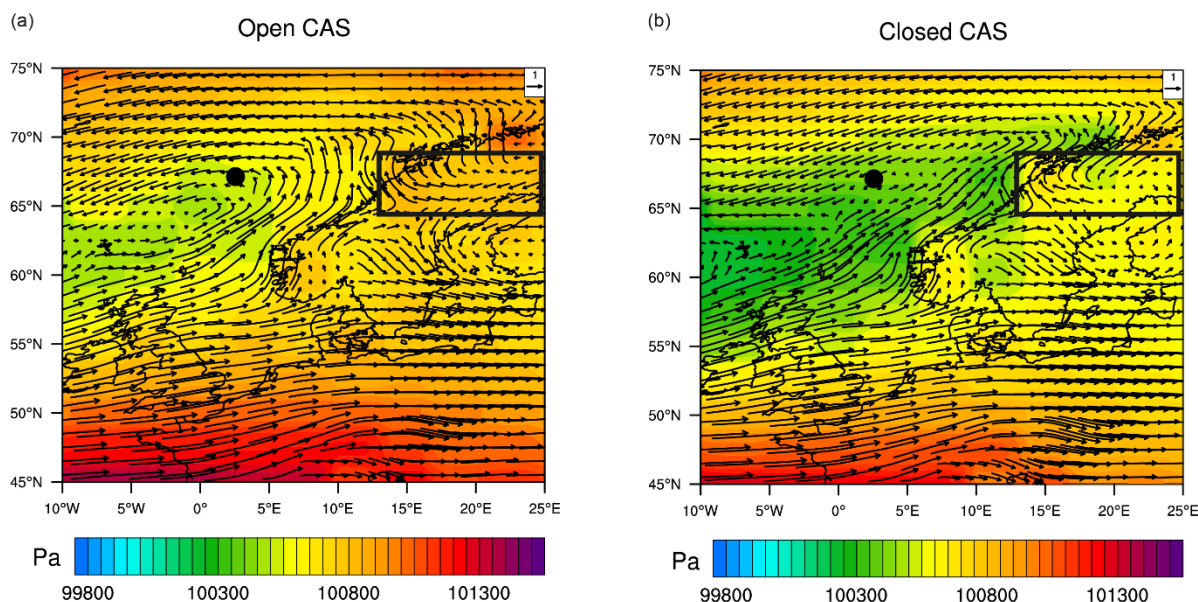


Figure 4: Model predictions for wind vectors (arrows, m s^{-1}) and mean sea level pressure (Pa) in spring (March, April, May) in the Nordic Seas region with an (a) open and (b) closed Central American Seaway (CAS). Black circle marks the location of ODP Hole 642B in the Norwegian Sea (67°N , 3°E). Black box shows an area in central/northern Scandinavia where the wind strength and direction changes significantly between the two simulations and is referred to within the main text.

359 To test the hypothesis of AMOC related atmospheric circulation changes affecting pollen
 360 transport to Hole 642B (potentially, but not uniquely, associated with a shoaling of the CAS),
 361 mean surface wind velocities during spring were compared from experiments with an OCAS
 362 and CCAS (Figure 4). In both experiments the predominant atmospheric flow in the Nordic
 363 Seas is westerly and south-westerly. However, the pattern of atmospheric circulation over the
 364 Scandinavian land mass is more complex. Of particular note, is the easterly flow moving out
 365 into the Nordic Seas over central and northern Scandinavia. This easterly flow is suppressed
 366 in the CCAS scenario, therefore we suggest that the potential for pollen transport from
 367 Scandinavia to Hole 642B is enhanced under weaker AMOC scenarios during the Pliocene
 368 (e.g. OCAS).

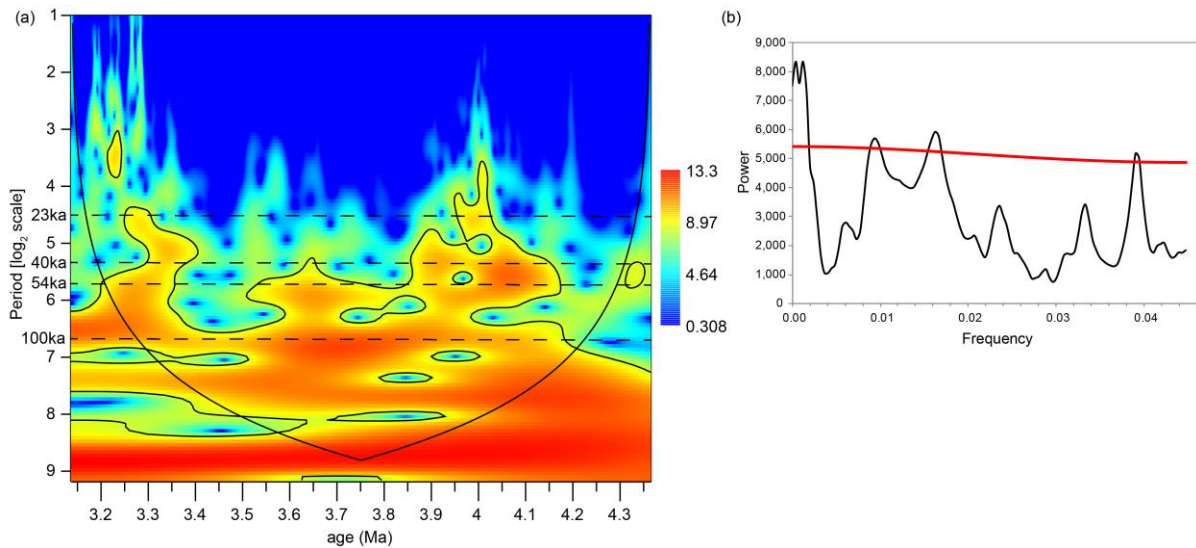
369 Whilst the timing of CAS closure is widely debated, our HadCM3 simulations suggest that a
 370 closing of the CAS could impact wind-fields over Norway (associated with an increase in the
 371 AMOC with a closing CAS). Therefore, this provides a potential explanation for part of the

372 decrease in PAR after 4.65 Ma, as this lies within the uncertainty related to the timing of
373 CAS closure (Haug et al., 2001; Steph et al., 2010). However, we also acknowledge that there
374 are other potential mechanisms (e.g. palaeogeographic changes in the Arctic; Otto-Bliesner et
375 al., 2017) that could cause a change in Pliocene AMOC and are not associated with the
376 closure of CAS, which could therefore affect pollen deposition at Hole 642B.

377 **5.2. Long-term cooling and climatic cyclicity**

378 The Pliocene pollen record from Hole 642B reveals four major changes in vegetation and
379 climate in northern Norway, with cooler, boreal conditions developing at 4.30 Ma and 3.47
380 Ma and warmer, cool temperate conditions at 3.90 Ma and 3.29 Ma (Figure 2). These
381 changes are indicative of repeated latitudinal shifts of the northern boundary of the deciduous
382 forest zone. Possible controls on the long-term vegetation changes in northern Norway
383 include declining atmospheric CO₂ concentrations and astronomical forcing.

384 Over the almost two-million-year-long record, the relative abundance of the thermophilic
385 taxon *Sciadopitys* shows a continuous decline during subsequent warm intervals (Figure 2).
386 At present, *Sciadopitys* is endemic to Japan where it thrives on well-drained slopes in a
387 temperate and wet climate (Ishikawa and Watanabe, 1986). During the Neogene, *Sciadopitys*
388 was a common element in the temperate forests of the Northern Hemisphere, forming part of
389 many different plant communities that inhabited diverse environments from lowland swamps
390 to high-altitude forests (e.g. Figueiral et al., 1999). In northern Norway, the decline of this
391 species throughout the Pliocene may be indicative of a progressive cooling of climate that is
392 also evident in other Pliocene terrestrial and marine records (e.g. Lawrence et al., 2009; Naafs
393 et al., 2010; Verhoeven et al., 2013). Decreasing atmospheric CO₂ concentrations have been



394

Figure 5: (a) Spectral analysis based on continuous wavelet transform of the relative abundance changes of *Pinus* pollen. Signal power is shown with a colour scale (red = higher). The black contour line indicates the significance level corresponding to $p=0.05$; and (b) REDFIT power spectrum (black line) testing whether peaks in the spectrum are significant against the red-noise background (Schulz and Mudelsee, 2002). False-alarm confidence level (red line) has been set to 90%.

395 suggested to be the main driver for the long-term cooling throughout the Pliocene leading to
 396 the onset of NHG (e.g. Lunt et al., 2008a; Martínez-Botí et al., 2015).

397 Continuous wavelet transform of *Pinus* pollen percentages reveals the influence of ~23-kyr
 398 precession, ~40 and 54-kyr obliquity for some intervals and relatively strong ~100-kyr
 399 eccentricity cycles (Figure 5). Low-frequency, large-amplitude changes linked to eccentricity
 400 could also be identified in the stable oxygen and carbon isotope records from Hole 642B
 401 (Risebrobakken et al., 2016). For the vegetation record, REDFIT identifies significance for
 402 the 100-kyr eccentricity, 54-kyr obliquity and the 23-kyr precession cycles (Figure 5). A
 403 dominance of precession cycles during the Pliocene has also been described from a
 404 compilation of Mediterranean SSTs and marine biomarker accumulation (Herbert et al.,
 405 2015). REDFIT could not identify significant 40-kyr obliquity cycles previously described
 406 from other marine sites in the North Atlantic for the Early and Late Pliocene (Figure 5)

407 (Lawrence et al., 2009; Naafs et al., 2010). However, it should be noted that the spectral and
408 power spectrum analysis of the Hole 642B pollen record is limited due to the unevenly
409 distributed sampling interval, which likely explains why wavelet transform could identify
410 obliquity and precession cycles in two, relatively densely sampled intervals only. While
411 astronomical forcing appears to be present in the Pliocene vegetation changes in northern
412 Norway, palaeogeographic and palaeoceanographic changes during the studied time interval
413 seem to have had a stronger influence on the long-term climate evolution of Scandinavia.

414 **5.3. Pliocene vegetation change and North Atlantic current variability**

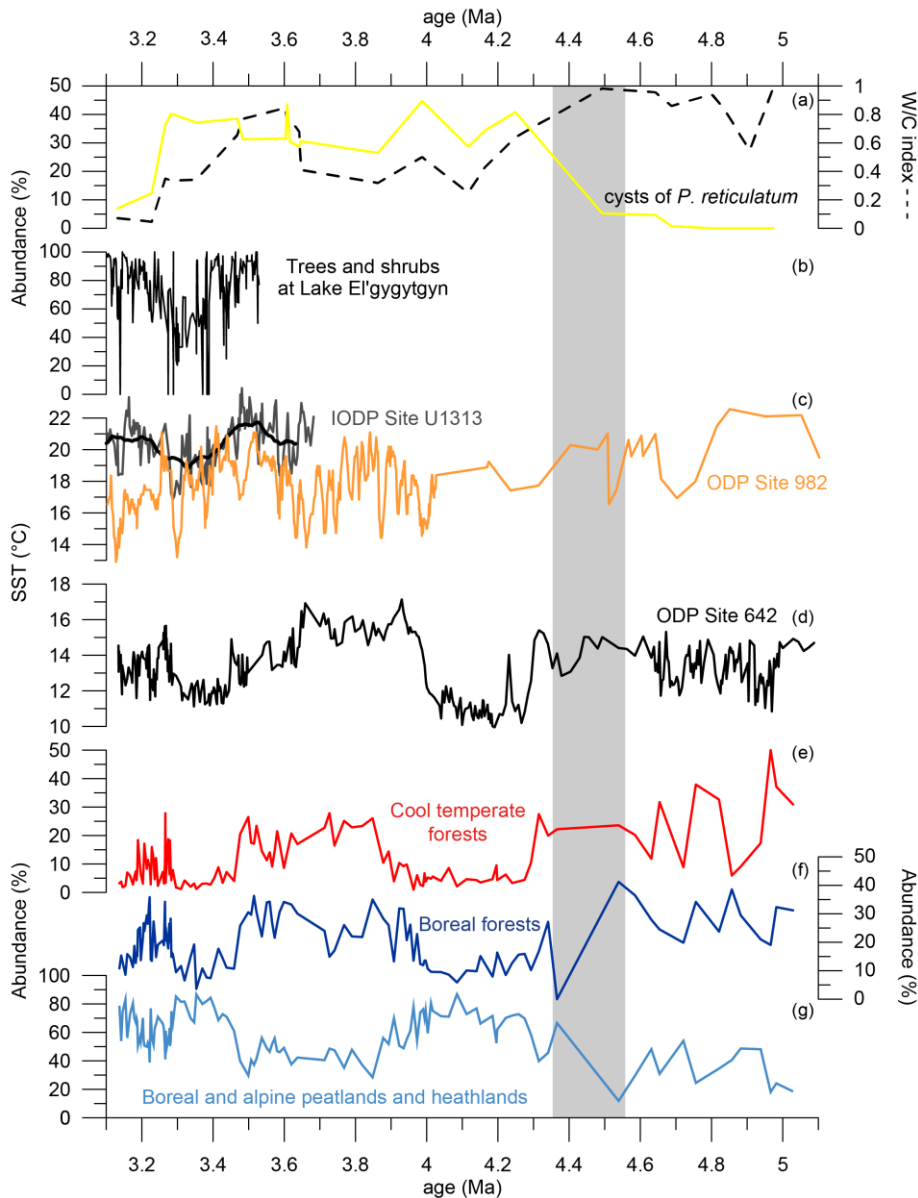
415 **5.3.1. Zanclean (5.3–3.6 Ma)**

416 During the early Zanclean (5.03–4.51 Ma), cool temperate deciduous to mixed forests
417 prevailed in northern Norway (Figure 2). Whether pure deciduous or mixed forests existed in
418 the lowlands of the Scandinavian mountains is not clear from the pollen signal due to the low
419 abundances of deciduous elements (see also Panitz et al., 2016). The latter is an artefact of
420 the distance of the site from the shore which also results in the over-representation of *Pinus*
421 pollen (e.g. Mudie and McCarthy, 2006). The presence of deciduous or mixed forests in
422 northern Norway suggests a northward shift of the northern limit of these forest zones by 4–
423 8° latitude, corresponding to an increase in average annual and July temperatures of at least
424 2–4°C and 4°C, respectively (Moen, 1999). A similar magnitude of warming is observed in
425 alkenone-derived SST estimates from Hole 642B, with SSTs up to ~3°C higher than the
426 Holocene average between 5.0 and 4.64 Ma (Figure 6) (Bachem et al., 2017). The alkenone-
427 derived SSTs are likely biased towards summer temperatures as the main growth period of
428 modern alkenone producing organisms occurs during the summer at higher altitudes due to
429 reduced incoming solar radiation during winter (Bachem et al., 2016 and references therein).
430 At ODP Site 982, which is situated in the path of the NAC before it enters the Norwegian

431 Sea, SSTs were ~6–12°C higher than present between 5.1 and 4.5 Ma (Figure 6) (Herbert et
432 al., 2016), indicating that warmer-than-present Atlantic water entered the Nordic Seas.

433 At c. 4.90–4.85 Ma, 4.72 Ma and 4.63 Ma, the establishment of boreal forests and the
434 development of peatlands at higher altitudes due to a lowering of the treeline are indicative of
435 cooler climatic conditions in northern Norway (Figure 2). Around 4.90–4.80 Ma, glacial
436 expansions have been inferred from ice-rafted debris (IRD) deposits in the Nordic Seas
437 (Fronval and Jansen, 1996; Jansen and Sjøholm, 1991; St. John and Krissek, 2002). In the
438 Norwegian Sea, IRD deposits point to the presence of sea-terminating glaciers around the
439 Nordic Seas at 4.9 Ma (Figure 3) (Bachem et al., 2017; Jansen et al., 1990). This cooling is
440 also recorded in alkenone-derived SST estimates from Hole 642B (Figure 6) (Bachem et al.,
441 2017). Dinocyst assemblages from Hole 642B reveal the influence of warm temperate
442 Atlantic water in the Norwegian Sea during the early Zanclean, but show a cooling in the
443 warm/cold index around 4.90 Ma (Figure 6) (De Schepper et al., 2015). At the same time,
444 enriched planktic and benthic $\delta^{18}\text{O}$ values suggest increased surface and bottom water
445 densities due to lower water temperatures (Risebrobakken et al., 2016). The cooling is also
446 evident in alkenone-based SSTs from ODP Site 907 in the Iceland Sea (De Schepper et al.,
447 2015; Herbert et al., 2016). The prevalence of mixed and boreal forests in northern Norway
448 around 4.90 Ma suggests that an extensive glaciation in Scandinavia is unlikely (Figure 2).
449 However, variable climatic conditions in northern Norway between 5.03 and 4.51 Ma are in
450 agreement with repeated cooling phases and related expansions of small-scale glaciations
451 around the Nordic Seas (Fronval and Jansen, 1996).

452 At Hole 642B, very low PARs occur between 4.56 and 4.37 Ma (Figure 2; see section 5.1 for
453 discussion). The pollen assemblage of the first sample above this interval is indicative of the
454 presence of boreal forests and tundra environments in northern Norway. This interpretation
455 should, however, be regarded with caution due to the low pollen counts. At 4.34 Ma, cool



456

457 **Figure 6:** Comparison of predominant vegetation and climate in northern Norway during the
 458 Pliocene to other Pliocene marine and terrestrial proxy records in the Northern Hemisphere.
 459 (a) relative abundance changes of the dinocyst cyst of *Protoceratium reticulatum* (yellow)
 460 and the warm (W)/cold (C) water index (De Schepper et al., 2015); (b) relative abundance
 461 changes of trees and shrubs at Lake El'gygytyn in NE Siberia (Andreev et al., 2014); (c)
 462 alkenone-derived sea surface temperature (SST) estimates at ODP Site 982 (orange) (Herbert
 463 et al., 2016; Lawrence et al., 2009) and IODP Site U1313 (grey) and the 100 kyr moving
 464 average (black) (Naafs et al., 2010); (d) SST estimates from ODP Hole 642B (Bachem et al.,
 465 2017); relative abundance changes of (e) cool temperate forest taxa, (f) boreal forest taxa and
 466 (g) boreal and alpine peatland and heathland taxa. For climatic grouping see Table 1. Grey
 467 bar highlights the interval with low pollen accumulation rates and counts.

468 temperate mixed forests indicate climate conditions similar to those before the interval with
469 low PARs. At 4.30 Ma, the development of herb fields/heathlands at higher altitudes,
470 followed by the expansion of peatlands at 4.15 Ma and the prevalence of boreal forests,
471 suggests cooler climatic conditions until 3.90 Ma (Figure 2). This cooling on land coincides
472 with the development of a modern-like NwAC between 4.50 and 4.30 Ma, as indicated by the
473 appearance of cysts of *Protoceratium reticulatum* and an increase in cool-water dinocysts,
474 that indicate a spread of cooler but still temperate waters across the Norwegian Sea (Figure 6)
475 (De Schepper et al., 2015). This is supported by planktic $\delta^{18}\text{O}$ values from Hole 642B which
476 indicate an increase in surface water salinities and/or cooling after 4.65 Ma (Risebrobakken et
477 al., 2016). Alkenone-derived SST estimates for Hole 642B show a cooling at 4.30 Ma (Figure
478 6), suggesting reduced northward heat transport via the NAC (Bachem et al., 2017). At Site
479 982 in the North Atlantic, a slight cooling between 4.3 and 4.0 Ma coincides with
480 reconstructed temperature changes at Hole 642B (Figure 6). However, it should be noted that
481 the full SST variability at Site 982 is likely not recorded due to the low temporal resolution
482 (see also Lawrence et al., 2009). At ODP Site 907 in the Iceland Sea, the gradual
483 disappearance of dinocyst species between 4.50 and 4.30 Ma likely reflects decreasing water
484 temperatures and salinity due to the establishment of a proto-EGC (Schreck et al., 2013). The
485 increased export of cool Arctic waters into the Nordic Seas via a modern-like EGC has been
486 linked to the prolonged establishment of northward water flow through the Bering Strait,
487 possibly as a result of the shoaling of the CAS (De Schepper et al., 2015; Schreck et al.,
488 2013; Verhoeven et al., 2011).

489 In northern Norway, diverse mixed forests and temperate climatic conditions re-established at
490 3.90 Ma (Figure 2). This warming is preceded by a rise in SSTs in the Norwegian Sea by
491 $\sim 6^\circ\text{C}$ between 4.0 and 3.93 Ma (Figure 6) (Bachem et al., 2017) and reduced surface water
492 densities (Risebrobakken et al., 2016), suggesting an increased inflow of warm Atlantic water

493 as a result of an enhanced northward heat transport, following the shoaling of the CAS (Steph
494 et al., 2010). The magnitude of warming seen in the Norwegian Sea (+ ~5°C compared to the
495 Holocene average) is comparable to an inferred increase of July temperatures of at least 4°C
496 in northern Norway, based on the latitudinal shift of vegetation zones (Moen, 1999). The
497 warming in northern Norway also coincides with the emergence of seasonal sea ice in the
498 Eurasian sector of the Arctic Ocean, with an increased sea ice export possibly
499 counterbalancing the northward heat transport via a stronger AMOC (Knies et al., 2014). This
500 is supported by Pliocene stable oxygen and carbon isotope records from Hole 642B, which
501 indicate the presence of a warmer NwAC and a vigorous upper water column circulation
502 between 4.0 and 3.65 Ma (Risebrobakken et al., 2016).

503 **5.3.2. Piacenzian (3.6–2.6 Ma)**

504 In northern Norway, temperate climatic conditions prevailed until 3.47 Ma (Figure 2),
505 corresponding to SSTs up to 6°C higher than present in the Norwegian Sea and North
506 Atlantic, indicating northward transport of warm Atlantic surface water (Figure 6) (Bachem
507 et al., 2017; Lawrence et al., 2009; Naafs et al., 2010). At Hole 642B, a sharp decline in the
508 relative abundance of coniferous trees and shrubs (excluding *Pinus*) between 3.48 and
509 3.46 Ma leads to the predominance of boreal forest and indicates a change towards subarctic
510 climate conditions in northern Norway. This cooling coincides with a distinct decrease in
511 alkenone-derived SST by ~2°C in the Norwegian Sea at 3.45 Ma (Figure 6) (Bachem et al.,
512 2017). There is also indications for an increase in surface water densities in response to
513 decreasing temperatures (Risebrobakken et al., 2016). A cooling is also recorded at Integrated
514 Ocean Drilling Program (IODP) Site U1313 at the north-eastern edge of the subtropical gyre
515 around 3.48–3.47 Ma (Figure 6) (Naafs et al., 2010). Following a brief warming at 3.45 Ma at
516 Site U1313, a subsequent gradual decline in SSTs suggests a weakened NAC and northward
517 heat transport (Naafs et al., 2010). A long-term cooling of alkenone-derived SSTs at ODP

518 Site 982 in the northern North Atlantic, starting at 3.5 Ma, is indicative of a gradual change of
519 climate before the intensification of NHG (Lawrence et al., 2009). At Site 982, obliquity-
520 driven high-amplitude SST variations during the Piacenzian are superimposed by a long-term
521 cooling trend (Figure 6). Lawrence et al. (2009) propose that the high amplitude variations at
522 Site 982 were caused by changes in the position of the westerlies as a result of orbitally
523 forced insolation changes, affecting the position of the NAC.

524 At 3.29 Ma, corresponding to the onset of warm climatic conditions during the mid-
525 Piacenzian (3.264–3.025 Ma), a return of cool temperate forests to northern Norway is in
526 agreement with an increase in alkenone-derived SSTs by $\sim 3^{\circ}\text{C}$ in the Norwegian Sea (Figure
527 6) (Bachem et al., 2017; Panitz et al., 2017). A decrease in surface water densities at the site
528 is also indicative of the presence of warmer waters in the Norwegian Sea (Risebrobakken et
529 al., 2016). A northward shift of the NAC and accompanied re-establishment of northward
530 heat transport is inferred from an increase in SSTs, and dinocyst assemblage changes around
531 3.29–3.28 Ma at several sites in the North Atlantic (De Schepper et al., 2013; Naafs et al.,
532 2010). In the Norwegian Sea, however, the warming is not associated with changes in
533 Atlantic water influence, suggesting that shifts in the position of the NAC are restricted to the
534 North Atlantic. Instead, the increase in marine and terrestrial temperatures coincides with an
535 increase in obliquity, resulting in a strengthening of the seasonal contrast (Panitz et al., 2017).
536 In the North Atlantic and Nordic Seas region, climatic conditions seem to be slightly colder
537 during the mid-Piacenzian than before 3.47 Ma, as seen in colder average SSTs at Site U1313
538 (Naafs et al., 2010), and a lower relative abundance of *Sciadopitys* pollen in the pollen
539 assemblages of Hole 642B (Figure 6). In the Norwegian Sea, SSTs are on average only 1°C
540 lower during the mid-Piacenzian than between 3.65 and 3.45 Ma (Figure 6) (Bachem et al.,
541 2017, 2016). An expansion of peatlands and decline in the prevalence of boreal forests in

542 northern Norway until 3.14 Ma are indicative of a cooling climate before the onset of NHG
543 around 2.7 Ma (Panitz et al., 2016).

544 In NE Siberia, a similar pattern to the climatic changes observed at Hole 642B and Site
545 U1313 is recorded in the relative abundance changes of trees and shrubs in the vicinity of
546 Lake El'gygytgyn (Figure 6) (Andreev et al., 2014). While the vegetation opens around
547 c. 3.47 Ma and c. 3.45 Ma, a pronounced decline in the relative abundance of trees and shrubs
548 does not take place until c. 3.39 Ma. Warmer conditions establish after c. 3.28 Ma, with
549 relative abundances of trees and shrubs accounting for >50% (Andreev et al., 2014). Changes
550 in vegetation and climate are also recorded in northwest Africa around 3.48 Ma, with warmer
551 and wetter conditions prevailing before and drier climatic conditions after 3.48 Ma (Leroy
552 and Dupont, 1997). The first extensive aridification in northwest Africa at 3.26 Ma
553 corresponds to the onset of the mid-Piacenzian, and is marked by the establishment of cool
554 temperate conditions in Norway. The similarity between the different Northern Hemisphere
555 records suggests that the observed climatic changes have a common forcing.

556 **6. Conclusions**

557 Our new high-resolution pollen record from ODP Hole 642B in the Nordic Seas enables the
558 reconstruction of long-term climate evolution in the Norwegian Arctic during the Pliocene.
559 The record shows multiple changes from warmer-than-present cool temperate to near-modern
560 boreal conditions which are superimposed by a long-term cooling trend throughout the
561 Pliocene. A comparison of vegetation changes with palaeoceanographic changes in the
562 Nordic Sea allowed the identification of different climate forcings: shifts to a warmer-than-
563 present Pliocene vegetation and climate with deciduous or mixed forests in northern Norway
564 (northward shift of 4–8° latitude, average annual and July temperatures > +2–4°C and 4°C,
565 respectively) correspond to enhanced northward heat transport via the NAC and NwAC,

566 whereas boreal vegetation and climate occurred when northward heat transport was weaker.
567 During the Early Pliocene, we suggest that a marked decline in PARs (c. 4.65 Ma) may have
568 been caused by oceanographic and atmospheric circulation changes. Climate model
569 experiments suggest that pollen transport to the site may have been reduced after c. 4.65 Ma
570 due to changes in the atmospheric circulation pattern linked to an enhanced AMOC. An
571 increase in AMOC might have been caused by the shoaling of the CAS between 4.8 and
572 4.2 Ma. A gradual decrease of relative abundances of *Sciadopitys* pollen over subsequent
573 warm phases suggests a long-term cooling of climate, possibly in response to declining
574 atmospheric CO₂ concentrations throughout the Pliocene. Astronomical forcing could also be
575 identified within the vegetation record, particularly a 100-kyr cycle. However, distinct
576 changes in vegetation and climate were linked to changes in the northward heat transport via
577 the NAC. Our Pliocene pollen record from Hole 642B suggests that palaeogeographic and
578 palaeoceanographic changes had a strong influence on the long-term climate evolution of
579 Scandinavia during the Pliocene. To further understand land-sea linkages and climate forcing
580 under warmer-than-present conditions, additional high-resolution studies along the
581 Scandinavian coast are required, recording the spatial extent of marine and terrestrial
582 environmental changes.

583 **7. Acknowledgements**

584 We would like to thank the International Ocean Drilling Program for providing the samples.
585 We acknowledge the work of M. Jones (Palynological Laboratory Services Ltd) and Lesley
586 Dunlop (Northumbria University) in helping with the preparation of samples. The work is
587 part of the “Ocean Controls on high-latitude Climate sensitivity – a Pliocene case study”
588 (OCCP) project funded by the Norwegian Research Council (project 221712). SDS also
589 acknowledges support from the Norwegian Research Council (project 229819). AMH and

590 AMD acknowledge that this work was completed in receipt of funding from the European
591 Research Council under the European Union's Seventh Framework Programme (FP7/2007–
592 2013)/ERC grant agreement no. 278636. We thank Paul Bachem for discussions of the results
593 that aided data interpretation. We are grateful for comments from T. H. Donders and
594 anonymous reviewer, which improved the manuscript.

595 **8. Declaration of interest**

596 Conflicts of interest: none.

597 **9. References**

- 598 Andreev, A.A., Tarasov, P.E., Wennrich, V., Raschke, E., Herzschuh, U., Nowaczyk, N.R.,
599 Brigham-Grette, J., Melles, M., 2014. Late Pliocene and Early Pleistocene vegetation
600 history of northeastern Russian Arctic inferred from the Lake El'gygytgyn pollen record.
601 *Clim. Past* 10, 1017–1039. doi:10.5194/cp-10-1017-2014
- 602 Bachem, P.E., Risebrobakken, B., De Schepper, S., McClymont, E.L., 2017. Highly variable
603 Pliocene sea surface conditions in the Norwegian Sea. *Clim. Past* 13, 1153–1168.
604 doi:10.5194/cp-13-1153-2017
- 605 Bachem, P.E., Risebrobakken, B., McClymont, E.L., 2016. Sea surface temperature
606 variability in the Norwegian Sea during the late Pliocene linked to subpolar gyre
607 strength and radiative forcing. *Earth Planet. Sci. Lett.* 446, 113–122.
608 doi:10.1016/j.epsl.2016.04.024
- 609 Bell, D.B., Jung, S.J.A., Kroon, D., Hodell, D.A., Lourens, L.J., Raymo, M.E., 2015. Atlantic
610 Deep-water Response to the Early Pliocene Shoaling of the Central American Seaway.
611 *Sci. Rep.* 5, 12252. doi:10.1038/srep12252
- 612 Bennike, O., Abrahamsen, N., Bak, M., Israelson, C., Konradi, P., Matthiessen, J.,
613 Witkowski, A., 2002. A multi-proxy study of Pliocene sediments from Île de France,
614 North-East Greenland. *Palaeogeogr. Palaeoclimatol. Palaeoecol.* 186, 1–23.
- 615 Beug, H.J., 2004. Leitfaden der Pollenbestimmung für Mitteleuropa und angrenzende
616 Gebiete. Dr. Friedrich Pfeil, München.
- 617 Bleil, U., 1989. 40. Magnetostratigraphy of Neogene and Quaternary Sediment Series from
618 the Norwegian Sea: Ocean Drilling Program, Leg 104. *Proc. Ocean Drill. Program, Sci.*
619 *Results* 104, 829–901.
- 620 De Schepper, S., Groeneveld, J., Naafs, B.D.A., Van Renterghem, C., Hennissen, J., Head,
621 M.J., Louwye, S., Fabian, K., 2013. Northern Hemisphere Glaciation during the
622 Globally Warm Early Late Pliocene. *PLoS One* 8, e81508.
623 doi:10.1371/journal.pone.0081508
- 624 De Schepper, S., Schreck, M., Beck, K., Matthiessen, J., 2015. Early Pliocene onset of
625 modern Nordic Seas circulation due to ocean gateway changes. *Nat. Commun.* 6, 1–8.
626 doi:10.1038/ncomms9659
- 627 de Vernal, A., Mudie, P.J., 1989a. Pliocene and Pleistocene palynostratigraphy at ODP Sites
628 646 and 647, eastern and southern Labrador Sea, in: *Proceedings of the Ocean Drilling*
629 *Program, Scientific Results.* Ocean Drilling Program College Station, Texas, pp. 401–
630 422.
- 631 de Vernal, A., Mudie, P.J., 1989b. Late Pliocene to Holocene palynostratigraphy at ODP Site
632 645, Baffin Bay, in: *Proceedings of the Ocean Drilling Program, Scientific Results.* pp.
633 387–399.
- 634 Dowsett, H.J., Barron, J.A., Poore, R.Z., Thompson, R.S., Cronin, T.M., Ishman, S.E.,
635 Willard, D.A., 1999. Middle Pliocene paleoenvironmental reconstruction: PRISM2.
636 USGS Open File Rep.

- 637 Dowsett, H.J., Foley, K.M., Stoll, D.K., Chandler, M.A., Sohl, L.E., Bentsen, M., Otto-
638 Bliesner, B.L., Bragg, F.J., Chan, W.-L., Contoux, C., Dolan, A.M., Haywood, A.M.,
639 Jonas, J.A., Jost, A., Kamae, Y., Lohmann, G., Lunt, D.J., Nisancioglu, K.H., Abe-
640 Ouchi, A., Ramstein, G., Riesselman, C.R., Robinson, M.M., Rosenbloom, N.A.,
641 Salzmann, U., Stepanek, C., Strother, S.L., Ueda, H., Yan, Q., Zhang, Z., 2013. Sea
642 Surface Temperature of the mid-Piacenzian Ocean: A Data-Model Comparison. *Sci.*
643 *Rep.* 3, 1–8. doi:10.1038/srep02013
- 644 Dupont, L., 2011. Orbital scale vegetation change in Africa. *Quat. Sci. Rev.* 30, 3589–3602.
645 doi:10.1016/j.quascirev.2011.09.019
- 646 Eidvin, T., Jansen, E., Rundberg, Y., Brekke, H., Grogan, P., 2000. The upper Cainozoic of
647 the Norwegian continental shelf correlated with the deep sea record of the Norwegian
648 Sea and the North Atlantic. *Mar. Pet. Geol.* 17, 579–600. doi:10.1016/S0264-
649 8172(00)00008-8
- 650 Eidvin, T., Riis, F., Rasmussen, E.S., 2014. Oligocene to Lower Pliocene deposits of the
651 Norwegian continental shelf, Norwegian Sea, Svalbard, Denmark and their relation to
652 the uplift of Fennoscandia: A synthesis. *Mar. Pet. Geol.* 56, 184–221.
653 doi:10.1016/j.marpetgeo.2014.04.006
- 654 Faegri, K., Iversen, J., 1989. *Textbook of Pollen Analysis*. Wiley&Sons, Chichester.
- 655 Faleide, J.I., Tsikalas, F., Breivik, A.J., Mjelde, R., Ritzmann, O., Øyvind, E., Wilson, J.,
656 Eldholm, O., 2008. Structure and evolution of the continental margin off Norway and
657 the Barents Sea. *Episodes* 31, 82–91.
- 658 Feng, R., Otto-bliesner, B.L., Fletcher, T.L., Tabor, C.R., Ballantyne, A.P., Brady, E.C.,
659 2017. Amplified Late Pliocene terrestrial warmth in northern high latitudes from greater
660 radiative forcing and closed Arctic Ocean gateways. *Earth Planet. Sci. Lett.* 466, 129–
661 138. doi:10.1016/j.epsl.2017.03.006
- 662 Figueiral, I., Mosbrugger, V., Rowe, N.P., Ashraf, A.R., Utescher, T., Jones, T.P., 1999. The
663 miocene peat-forming vegetation of northwestern Germany: An analysis of wood
664 remains and comparison with previous palynological interpretations. *Rev. Palaeobot.*
665 *Palynol.* 104, 239–266. doi:10.1016/S0034-6667(98)00059-1
- 666 Fronval, T., Jansen, E., 1996. Late Neogene paleoclimates and paleoceanography in the
667 Iceland-Norwegian Sea: evidence from the Iceland and Vøring Plateaus. *Proc. Ocean*
668 *Drill. Program, Sci. Results* 151, 455–468.
- 669 Furevik, T., 2000. Large-scale atmospheric circulation variability and its impacts on the
670 Nordic seas ocean climate: A review. *Nord. Seas An Integr. Perspect. Geophys. Monogr.*
671 *Ser.* 158, 105–136.
- 672 Gordon, C., Cooper, C., Senior, C.A., Banks, H., Gregory, J.M., Johns, T.C., Mitchell, J.F.B.,
673 Wood, R.A., 2000. The simulation of SST, sea ice extents and ocean heat transports in a
674 version of the Hadley Centre coupled model without flux adjustments. *Clim. Dyn.* 16,
675 147–168. doi:10.1007/s003820050010
- 676 Grimm, E.C., 1990. TILIA and TILIA* GRAPH. PC spreadsheet and graphics software for
677 pollen data. *INQUA, Work. Gr. Data-Handling Methods Newsl.* 4, 5–7.

- 678 Grimm, E.C., 1987. CONISS: a FORTRAN 77 program for stratigraphically constrained
679 cluster analysis by the method of incremental sum of squares. *Comput. Geosci.* 13, 13–
680 35.
- 681 Groeneveld, J., Nürnberg, D., Tiedemann, R., Reichart, G.-J., Steph, S., Reuning, L., Crudeli,
682 D., Mason, P.R.D., 2008. Foraminiferal Mg/Ca increase in the Caribbean during the
683 Pliocene: Western Atlantic Warm Pool formation, salinity influence, or diagenetic
684 overprint? *Geochemistry, Geophys. Geosystems* 9, GC1564.
685 doi:10.1029/2006GC001564
- 686 Haug, G.H., Tiedemann, R., Zahn, R., Ravelo, A.C., 2001. Role of Panama uplift on oceanic
687 freshwater balance. *Geology* 29, 207–210. doi:10.1130/0091-
688 7613(2001)029<0207:ROPUOO>2.0.CO;2
- 689 Haywood, A.M., Hill, D.J., Dolan, A.M., Otto-Bliesner, B.L., Bragg, F., Chan, W.-L.,
690 Chandler, M.A., Contoux, C., Dowsett, H.J., Jost, A., Kamae, Y., Lohmann, G., Lunt,
691 D.J., Abe-Ouchi, A., Pickering, S.J., Ramstein, G., Rosenbloom, N.A., Salzmann, U.,
692 Sohl, L., Stepanek, C., Ueda, H., Yan, Q., Zhang, Z., 2013. Large-scale features of
693 Pliocene climate: results from the Pliocene Model Intercomparison Project. *Clim. Past* 9,
694 191–209. doi:10.5194/cp-9-191-2013
- 695 Haywood, A.M., Valdes, P.J., 2004. Modelling Pliocene warmth: contribution of atmosphere,
696 oceans and cryosphere. *Earth Planet. Sci. Lett.* 218, 363–377.
- 697 Herbert, T.D., Lawrence, K.T., Tzanova, A., Peterson, L.C., Caballero-Gill, R., Kelly, C.S.,
698 2016. Late Miocene global cooling and the rise of modern ecosystems. *Nat. Geosci.* 9,
699 843–849. doi:10.1038/ngeo2813
- 700 Herbert, T.D., Ng, G., Cleaveland Peterson, L., 2015. Evolution of Mediterranean sea surface
701 temperatures 3.5–1.5 Ma: Regional and hemispheric influences. *Earth Planet. Sci. Lett.*
702 409, 307–318. doi:10.1016/j.epsl.2014.10.006
- 703 Hilgen, F.J., Lourens, L.J., Van Dam, J.A., 2012. Chapter 29 - The Neogene Period, in: *The*
704 *Geologic Time Scale*. Elsevier, Burlington, MA, USA, pp. 923–978. doi:10.1016/B978-
705 0-444-59425-9.00029-9
- 706 Hill, D.J., 2015. The non-analogue nature of Pliocene temperature gradients. *Earth Planet.*
707 *Sci. Lett.* 425, 232–241. doi:10.1016/j.epsl.2015.05.044
- 708 Ishikawa, S., Watanabe, N., 1986. An ecological study on the *Sciadopitys verticillata* forest
709 and other natural forests of Mt. Irazu, southern Shikoku, Japan. *Mem. - Fac. Sci. Kochi*
710 *Univ. Ser. D Biol.* 7, 63–66.
- 711 Jansen, E., Sjøholm, J., 1991. Reconstruction of Glaciation over the Past 6 Myr from Ice-
712 Borne Deposits in the Norwegian Sea. *Lett. to Nat.* 349, 600–603.
- 713 Jansen, E., Sjøholm, J., Bleil, U., Erichsen, J., 1990. Neogene and Pleistocene glaciations in
714 the northern hemisphere and late Miocene - Pliocene global ice volume fluctuations:
715 evidence from the Norwegian Sea, in: *Geological History of the Polar Oceans: Arctic*
716 *versus Antarctic*. Springer Netherlands, pp. 677–705.
- 717 Knies, J., Cabedo-Sanz, P., Belt, S.T., Baranwal, S., Fietz, S., Rosell-Melé, A., 2014. The
718 emergence of modern sea ice cover in the Arctic Ocean. *Nat. Commun.* 5, 5608.

- 719 doi:10.1038/ncomms6608
- 720 Lawrence, K.T., Herbert, T.D., Brown, C.M., Raymo, M.E., Haywood, A.M., 2009. High-
721 amplitude variations in North Atlantic sea surface temperature during the early Pliocene
722 warm period. *Paleoceanography* 24, PA2218. doi:10.1029/2008PA001669
- 723 Leroy, S.A.G., Dupont, L.M., 1997. Marine palynology of the ODP Site 658 (N-W Africa)
724 and its contribution to the stratigraphy of late Pliocene. *GEOBIOS* 30, 351–359.
- 725 Lisiecki, L.E., Raymo, M.E., 2005. A Pliocene-Pleistocene stack of 57 globally distributed
726 benthic $\delta^{18}\text{O}$ records. *Paleoceanography* 20, PA1003.
- 727 Lunt, D.J., Foster, G.L., Haywood, A.M., Stone, E.J., 2008a. Late Pliocene Greenland
728 glaciation controlled by a decline in atmospheric CO₂ levels. *Nature* 454, 1102–1105.
- 729 Lunt, D.J., Valdes, P.J., Haywood, A., Rutt, I.C., 2008b. Closure of the Panama Seaway
730 during the Pliocene: implications for climate and Northern Hemisphere glaciation. *Clim.*
731 *Dyn.* 30, 1–18. doi:10.1007/s00382-007-0265-6
- 732 Martínez-Botí, M.A., Foster, G.L., Chalk, T.B., Rohling, E.J., Sexton, P.F., Lunt, D.J.,
733 Pancost, R.D., Badger, M.P.S., Schmidt, D.N., 2015. Plio-Pleistocene climate sensitivity
734 evaluated using high-resolution CO₂ records. *Nature* 518, 49–54.
735 doi:10.1038/nature14145
- 736 McCarthy, F.M.G., Gostlin, K.E., Mudie, P.J., Hopkins, J.A., 2003. Terrestrial and Marine
737 Palynomorphs As Sea-Level Proxies : an Example From Quaternary Sediments on the
738 New Jersey Margin , U . S . a . Soc. Sediment. Geol. 119–129.
- 739 McCarthy, F.M.G., Mudie, P.J., 1998. Oceanic pollen transport and pollen:dinocyst ratios as
740 markers of late Cenozoic sea level change and sediment transport. *Palaeogeogr.*
741 *Palaeoclimatol. Palaeoecol.* 138, 187–206. doi:10.1016/S0031-0182(97)00135-1
- 742 Moen, A., 1999. National Atlas of Norway: vegetation. Norwegian Mapping Authority,
743 Hønefoss, Norway.
- 744 Moen, A., 1987. The regional vegetation of Norway; that of central Norway in particular.
745 *Nord. Geogr. Tidsskr.* 41, 179–226.
- 746 Mork, M., 1981. Circulation phenomena and frontal dynamics of the Norwegian coastal
747 current. *Philos. Trans. R. Soc. London* 302, 635–647.
- 748 Mudie, P.J., McCarthy, F.M.G., 2006. Marine palynology: potentials for onshore - offshore
749 correlation of Pleistocene - Holocene records. *Trans. R. Soc. South Africa* 61, 139–157.
- 750 Naafs, B.D.A., Stein, R., Hefter, J., Khélifi, N., De Schepper, S., Haug, G.H., 2010. Late
751 Pliocene changes in the North Atlantic Current. *Earth Planet. Sci. Lett.* 298, 434–442.
752 doi:10.1016/j.epsl.2010.08.023
- 753 Orvik, K.A., Niiler, P., 2002. Major pathways of Atlantic water in the northern North Atlantic
754 and Nordic Seas toward Arctic. *Geophys. Res. Lett.* 29, 2-1-2-4.
755 doi:10.1029/2002GL015002
- 756 Osborne, A.H., Newkirk, D.R., Groeneveld, J., Martin, E.E., Tiedemann, R., Frank, M., 2014.
757 The seawater neodymium and lead isotope record of the final stages of Central

- 758 American Seaway closure. *Paleoceanography* 29, 715–729. doi:10.1002/2014PA002676
- 759 Otto-Bliesner, B.L., Jahn, A., Feng, R., Brady, E.C., Hu, A., Löffverström, M., 2017.
760 Amplified North Atlantic warming in the late Pliocene by changes in Arctic gateways.
761 *Geophys. Res. Lett.* 44, 957–964. doi:10.1002/2016GL071805
- 762 Panitz, S., De Schepper, S., Salzmann, U., Bachem, P.E., Risebrobakken, B., Clotten, C.,
763 Hocking, E.P., 2017. Mid-Piacenzian variability of Nordic Seas surface circulation
764 linked to terrestrial climatic change in Norway. *Paleoceanography* 32, PA003166.
765 doi:10.1002/2017PA003166
- 766 Panitz, S., Salzmann, U., Risebrobakken, B., De Schepper, S., Pound, M.J., 2016. Climate
767 variability and long-term expansion of peatlands in Arctic Norway during the late
768 Pliocene (ODP Site 642, Norwegian Sea). *Clim. Past* 12, 1043–1060. doi:10.5194/cpd-
769 11-5755-2015
- 770 Raymo, M.E., Grant, B., Horowitz, M., Rau, G.H., 1996. Mid-Pliocene warmth: stronger
771 greenhouse and stronger conveyor. *Mar. Micropaleontol.* 27, 313–326.
772 doi:10.1016/0377-8398(95)00048-8
- 773 Raymo, M.E., Hodell, D., Jansen, E., 1992. Response of deep ocean circulation to initiation
774 of Northern Hemisphere glaciation (3–2 Ma). *Paleoceanography* 7, 645–672.
775 doi:10.1029/92pa01609
- 776 Risebrobakken, B., Andersson, C., De Schepper, S., McClymont, E.L., 2016. Low frequency
777 Pliocene climate variability on the eastern Nordic Seas. *Paleoceanography* 31, 1154–
778 1175. doi:10.1002/2015PA002918
- 779 Salzmann, U., Dolan, A.M., Haywood, A.M., Chan, W.-L., Voss, J., Hill, D.J., Abe-Ouchi,
780 A., Otto-Bliesner, B., Bragg, F.J., Chandler, M.A., Contoux, C., Dowsett, H.J., Jost, A.,
781 Kamae, Y., Lohmann, G., Lunt, D.J., Pickering, S.J., Pound, M.J., Ramstein, G.,
782 Rosenbloom, N.A., Sohl, L., Stepanek, C., Ueda, H., Zhang, Z., 2013. Challenges in
783 quantifying Pliocene terrestrial warming revealed by data-model discord. *Nat. Clim.*
784 *Chang.* 3, 969–974.
- 785 Schreck, M., Meheust, M., Stein, R., Matthiessen, J., 2013. Response of marine
786 palynomorphs to Neogene climate cooling in the Iceland Sea (ODP Hole 907A). *Mar.*
787 *Micropaleontol.* 101, 49–67. doi:10.1016/j.marmicro.2013.03.003
- 788 Schulz, M., Mudelsee, M., 2002. REDFIT: Estimating red-noise spectra directly from
789 unevenly spaced paleoclimatic time series. *Comput. Geosci.* 28, 421–426.
790 doi:10.1016/S0098-3004(01)00044-9
- 791 Shipboard Scientific Party, 1987. 4. Site 642: Norwegian Sea, in: Eldholm, O., Thiede, J.,
792 Taylor, E. (Eds.), . *Init. Repts.*, 104: College Station, TX (Ocean Drilling Program), pp.
793 53–453.
- 794 St. John, K.E.K., Krissek, L.A., 2002. The late Miocene to Pleistocene ice-rafting history of
795 southeast Greenland. *Boreas* 28–35.
- 796 Steph, S., Tiedemann, R., Prange, M., Groeneveld, J., Schulz, M., Timmermann, A.,
797 Nürnberg, D., Rühlemann, C., Saukel, C., Haug, G.H., 2010. Early Pliocene increase in
798 thermohaline overturning: A precondition for the development of the modern equatorial

- 799 Pacific cold tongue. *Paleoceanography* 25, 1–17. doi:10.1029/2008PA001645
- 800 Stockmarr, J., 1971. Tablets with spores used in absolute pollen analysis. *Pollen et spores* 13,
801 615–621.
- 802 Torrence, C., Compo, G. ~P. G.P., 1998. A practical guide to wavelet analysis. *Bull. Am.*
803 *Meteorol. Soc.* 79, 61–78. doi:10.1175/1520-0477(1998)079<0061:APGTWA>2.0.CO;2
- 804 Traverse, A., 1988. Production, dispersal, and sedimentation of spores/pollen, in:
805 *Paleopalynology*. UNWIN HYMAN, London, pp. 375–430.
- 806 Utescher, T., Dreist, A., Henrot, A.-J., Hickler, T., Liu, Y.-S.C., Mosbrugger, V., Portmann,
807 F.T., Salzmann, U., 2017. Continental climate gradients in North America and Western
808 Eurasia before and after the closure of the Central American Seaway. *Earth Planet. Sci.*
809 *Lett.* 472, 120–130.
- 810 Verhoeven, K., Louwye, S., Eiríksson, J., 2013. Plio-Pleistocene landscape and vegetation
811 reconstruction of the coastal area of the Tjörnes Peninsula, Northern Iceland. *Boreas* 42,
812 108–122. doi:10.1111/j.1502-3885.2012.00279.x
- 813 Verhoeven, K., Louwye, S., Eiríksson, J., De Schepper, S., 2011. A new age model for the
814 Pliocene-Pleistocene Tjörnes section on Iceland: Its implication for the timing of North
815 Atlantic-Pacific palaeoceanographic pathways. *Palaeogeogr. Palaeoclimatol. Palaeoecol.*
816 309, 33–52. doi:10.1016/j.palaeo.2011.04.001
- 817 Willard, D.A., 1996. Pliocene-Pleistocene pollen assemblages from the Yermak Plateau,
818 Arctic Ocean: Sites 910 and 911. *Proc. Ocean Drill. Program, Sci. Results* 151, 297–
819 305.
- 820 Willard, D.A., 1994. Palynological record from the North Atlantic region at 3 Ma:
821 vegetational distribution during a period of global warmth. *Rev. Palaeobot. Palynol.* 83,
822 275–297. doi:10.1016/0034-6667(94)90141-4
- 823 Zhang, Z.S., Nisancioglu, K.H., Chandler, M.A., Haywood, A.M., Otto-Bliesner, B.L.,
824 Ramstein, G., Stepanek, C., Abe-Ouchi, A., Chan, W.L., Bragg, F.J., Contoux, C.,
825 Dolan, A.M., Hill, D.J., Jost, A., Kamae, Y., Lohmann, G., Lunt, D.J., Rosenbloom,
826 N.A., Sohl, L.E., Ueda, H., 2013. Mid-Pliocene Atlantic Meridional Overturning
827 Circulation not unlike modern. *Clim. Past* 9, 1495–1504. doi:10.5194/cp-9-1495-2013
- 828